

## Dark breathers in Klein-Gordon lattices. Band analysis of their stability properties.

A Alvarez †, JFR Archilla ‡, J Cuevas ‡ and FR Romero †

Nonlinear Physics Group of the University of Sevilla.

†Facultad de Física, P. 5 and ‡Dep. Física Aplicada I en ETSI Informática.

Avda. Reina Mercedes s/n, 41012 Sevilla, Spain.

**Abstract.** Discrete bright breathers are well known phenomena. They are localized excitations that consist of a few excited oscillators in a lattice and the rest of them having very small amplitude or none. In this paper we are interested in the opposite kind of localization, or discrete dark breathers, where most of the oscillators are excited and one or a few units of them have very small amplitude. We investigate using band analysis, Klein-Gordon lattices at frequencies not close to the linear ones. Dark breathers at low coupling are shown to be stable for Klein-Gordon chains with soft on-site potentials and repulsive dispersive interaction, and with hard on-site potentials and attractive dispersive interactions. At higher coupling dark breathers lose their stability via subharmonic, harmonic or oscillatory bifurcations, depending on the model. However, most of these bifurcations are harmless in the sense that they preserve dark localization. None of these bifurcations disappear when the system is infinite. Dark breathers in dissipative systems are found to be stable for both kinds of dispersive interaction.

PACS numbers: 63.20.Pw, 63.20.Ry, 66.90.+r,

## 1. Introduction

It is well known that intrinsic localized modes (also called *discrete breathers*) are exact, periodic and localized solutions that can be obtained in a large variety of nonlinear discrete systems. They are becoming a new paradigm for understanding many aspects of the behaviour of discrete systems (for a review, see, e.g., [1, 2]). Mackay and Aubry [3] proved analytically their existence and the conditions for their stability [1], under rather general hypotheses. Since then, many accurate numerical methods have been used to obtain breathers as exact numerical solutions up to machine precision [4], which permits the analysis of breathers properties. Thus, for a given model, it is possible to perform a numerical study of the ranges of existence and stability in the parameters space.

The term discrete breather is usually understood as a localized, periodic solution in a discrete system, but with a small number of excited oscillators. When only one oscillator has large amplitude it is known as *one-site breather*. When more than one oscillator have large amplitude, the term *multibreather* is used. Hereafter, we will use the term *bright breather* when there are one or a few oscillators vibrating with large amplitude whereas the rest of them oscillate with small amplitude.

However, localization can be manifested in a different way, which consists of all the oscillators vibrating with large amplitude except one or a few of them oscillating with very small amplitude. The natural name for these entities is *dark breathers*, analogously to the well known term *dark solitons*. For the nonlinear Schrödinger equations, which governs both nonlinear optical modes in fibers and dilute Bose–Einstein condensates, two different kinds of scalar soliton solutions, *bright and dark*, are known [5, 6]. Thus, a dark soliton is a solution which has a point with zero amplitude, that is, a soliton defining the absence of matter or energy. Since then, many papers have appeared referring to theoretical and experimental results referred to this entities. The effects of discreteness on the properties and propagation dynamics of dark solitons has been analyzed in the discrete nonlinear Schrödinger equation (DNLS), which is thought to be a good approximation for frequencies close to the linear frequency [7, 8, 9, 10, 11], the last one, also with numerics on actual Klein–Gordon systems. It is worth remarking that some examples of dark localization have been observed experimentally [12], and some structural properties have been analyzed in [13].

In this paper, we perform an analysis of the existence and stability of dark breathers for different models based on the properties of the band structure of the Newton operator. We have found that there exist stable dark breathers for a variety of one-dimensional Klein-Gordon lattices. For soft on-site potentials, dark breathers are stable only for repulsive dispersive interaction and for hard on-site potentials the stability founded is for attractive interaction. This results agree with the ones that have been found for the DNLS approximation in [14] as a consequence of the modulational instability of the constant amplitude background.

It is not clear in which physical systems dark breathers can play a significant role. A possibility is DNA, we conjecture that dark breathers can occur in DNA chains at high temperature, close to thermal denaturation [15]. In this situation, a great number of molecules are vibrating with high amplitude, whereas a few of them could be almost at rest.

This paper is organized as follows: In section 2, we describe the proposed Klein-Gordon models and the resulting evolution equations. In Section 3, we expose the tools

for calculating dark breathers, and we explicitly show that the theorem of existence of Mackay and Aubry gives an affirmative answer to the question of existence of dark breathers. In section 4, we expose the method for the analysis of the linear stability of breather solutions using both the Floquet multipliers and Aubry band's theory. In Section 5, we investigate the stability of dark breathers for chains with soft on-site potential and attractive interactions between the particles. We show that it is not possible to obtain stable dark breathers for every value of the coupling parameter. This negative result suggested us to consider the study of chains with repulsive interactions between particles. Our results confirm that in this case there exist stable dark breathers up to significant values of the coupling. In Section 6, lattices with hard on-site potentials are considered. For these cases, dark breathers are stable provided that particles interact through an attractive potential. Dark breathers become unstable through subharmonic, harmonic and oscillatory bifurcations depending on the type of the on-site potential. In section 7, we show that both subharmonic and oscillatory bifurcations do not disappear in infinite systems. The paper concludes with a short summary of the main results and some prospective in Section 9.

## 2. Models

We study one-dimensional, anharmonic, Hamiltonian lattices of the Klein–Gordon type. The Hamiltonian is given by

$$H = \sum_n \left( \frac{1}{2} \dot{u}_n^2 + V(u_n) \right) + \varepsilon W(u) \quad (1)$$

where  $u_n$  are the coordinates of the oscillators referred to their equilibrium positions;  $V(u_n)$  represents the on-site potential;  $u$  represents the set of variables  $\{u_n\}$ ; and  $\varepsilon W(u)$  represents the coupling potential, with  $\varepsilon$  being a parameter that describes the strength of the coupling. We suppose initially that  $\varepsilon$  is positive and  $W(u)$  is given by

$$W(u) = \frac{1}{2} \sum_n (u_{n+1} - u_n)^2. \quad (2)$$

This interaction is attractive because a nonzero value of a variable tends to increase the values of the neighbouring variables with the same sign. The on-site potential is given by

$$V(u_n) = \frac{1}{2} \omega_0^2 u_n^2 + \phi(u_n) \quad (3)$$

with  $\phi(u_n)$  being the anharmonic part of the potential. The variables are scaled so that all the particles in the lattice have mass unity and the linear frequency  $\omega_0 = 1$ . The dynamical equations for this system are

$$\ddot{u}_n + \omega_0^2 u_n + \phi'(u_n) + \varepsilon(2u_n - u_{n-1} - u_{n+1}) = 0. \quad (4)$$

These equations do not have analytical solutions and must be solved numerically. The solutions depend obviously on the chosen potentials  $V(u_n)$  and  $W(u)$ . We will analyze the system for several  $V(u_n)$  and coupling interactions  $W(u)$ . These models appear in many physical systems, a known example, with a suitable on-site potential  $V(u_n)$  is the Peyrard–Bishop model for DNA [15], where the variables  $u_n$  represent the stretching of the base pairs.

### 3. Dark breathers existence

We look for spatially localized, time-reversible and time-periodic solutions of equations (4) with a given frequency  $\omega_b$  and a continuous second derivative. Therefore, the functions  $u_n(t)$  can be obtained up to machine precision by truncated Fourier series of the form

$$u_n(t) = z_0 + \sum_{k=1}^{k=k_m} 2z_n^k \cos(k\omega_b t). \quad (5)$$

We distinguish three types of solutions of the isolated oscillators that can be coded in the following way:  $\sigma_n = 0$  for an oscillator at rest ( $u_n(t) = 0, \forall t$ );  $\sigma_n = +1$  for an excited oscillator with frequency  $\omega_b$  and  $u_n(0) > 0$ ; finally,  $\sigma_n = -1$  for an excited oscillator with frequency  $\omega_b$  and  $u_n(0) < 0$ . Time-reversible solutions of the whole system at  $\varepsilon = 0$  (anticontinuous limit), can be referred to by a coding sequence  $\sigma = \{\sigma_n\}$ . Therefore,  $\sigma = \{0, \dots, 0, 1, 0, \dots, 0\}$  corresponds to a one-site breather. Other codes can be  $\sigma = \{0, \dots, 0, 1, 1, 0, \dots, 0\}$  for a symmetric two-site breather, and  $\sigma = \{1, \dots, 1, 0, 1, \dots, 1\}$  for a one-site dark breather (this case correspond to the background in phase).

The method for calculating dark breathers is based on the general methods for obtaining breathers [4, 16, 17, 18, 19].

The existence theorem by MacKay and Aubry [3] establishes that every solution at the anticontinuous limit, corresponding to a code sequence can be continued up to a certain value of the coupling parameter  $\varepsilon_c \neq 0$ , as long as the following two hypotheses are fulfilled:

- The orbits of the uncoupled excited oscillators with the chosen frequency have to be such that  $\frac{\partial \omega_b}{\partial I} \neq 0$ , where  $I = \int p dq$  is the action variable of the oscillator. That is, the oscillator is truly nonlinear at that frequency.
- The frequency of the orbit must be such that  $p\omega_b \neq \omega_0$  for any integer  $p$ . That is, none of the breather harmonics coincide with the linear frequency  $\omega_0$ .

Therefore, this theorem gives an immediate answer to the question of the existence of dark breathers as they are obtained by continuation of the configuration mentioned above  $\sigma = \{1, \dots, 1, 0, 1, \dots, 1\}$ . However, the theorem does not give an estimate for the value of the coupling  $\varepsilon_c$  where the dark breather ceases to exist. Dark breathers have to be calculated numerically for each value of the coupling parameter, also it is worth investigating whether dark breathers are stable or not, and if they are stable, up to which value of the coupling parameter.

### 4. Dark breathers stability

The stability analysis of a given breather solution can be performed numerically [1, 19, 20, 21]. The linearized equations corresponding to perturbations of this solution are

$$\ddot{\xi}_n + \omega_0^2 \xi_n + \phi''(u_n) \xi_n + \varepsilon(2\xi_n - \xi_{n-1} - \xi_{n+1}) = 0 \quad (6)$$

where  $\xi = \{\xi_n(t)\}$  represents a small perturbation of the solution of the dynamical equations,  $u(t) = \{u_n(t)\}$ . The linear stability of these solutions can be studied by finding the eigenvalues of the Floquet matrix  $\mathcal{F}_0$ , called Floquet multipliers. The Floquet matrix transforms the column matrix with elements given by  $\xi_n(0)$

and  $\pi(0) \equiv \dot{\xi}_n(0)$  into the corresponding column matrix with elements  $\xi_n(T_b)$  and  $\pi(T_b) \equiv \dot{\xi}_n(T_b)$  for  $n = 1 \dots m$  and  $T_b = 2\pi/\omega_b$ , that is

$$\begin{pmatrix} \{\xi_n(T_b)\} \\ \{\pi_n(T_b)\} \end{pmatrix} = \mathcal{F}_0 \begin{pmatrix} \{\xi_n(0)\} \\ \{\pi_n(0)\} \end{pmatrix} \quad (7)$$

The Floquet matrix  $\mathcal{F}_0$  can be obtained numerically by integrating equations (6) a breather period. In order to get accurate results [22], we have used a symplectic integrator. Equation (6) can be written as an eigenvalue equation

$$(\mathcal{N}(u(t), \varepsilon) \cdot \xi)_n = E \xi_n \quad (8)$$

where  $\mathcal{N}(u(t), \varepsilon)$  is called the Newton operator. The solutions of equation (6) can be described as the eigenfunctions of  $\mathcal{N}$  for  $E = 0$ . The fact that the linearized system is Hamiltonian and real implies that the Floquet operator is a real and symplectic operator. The consequence is that if  $\lambda$  is an eigenvalue, then  $1/\lambda$ ,  $\lambda^*$  and  $1/\lambda^*$  are also eigenvalues, and therefore a necessary condition for linear stability is that every eigenvalue has modulus one, that is, they are located at the unit circle in the complex plane. Besides, there is always a double eigenvalue at  $1 + 0i$  from the fact that the derivative  $\{\dot{u}_n(t)\}$  is always a solution of (8) with  $E = 0$ .

The Floquet multipliers at the anticontinuous limit ( $\varepsilon = 0$ ) can be easily obtained for bright and dark breathers. If an oscillator at rest is considered, equation (6) becomes

$$\ddot{\xi}_n + \omega_0^2 \xi_n = 0 \quad (9)$$

with solution  $\xi(t) = \xi_0 e^{i\omega_0 t}$ , and therefore, the corresponding eigenvalue of  $\mathcal{F}_0$  is  $\lambda = \exp(i2\pi\omega_0/\omega_b)$ . If an oscillator is excited, equation (6) becomes

$$\ddot{\xi}_n + \omega_0^2 \xi_n + \phi''(u_n) \xi_n = 0. \quad (10)$$

This equation has  $\dot{u}_n(t)$  as a solution, which is periodic and therefore with Floquet multiplier  $\lambda = 1$ . Thus, for a bright breather, we have, taking into account their multiplicity,  $2(N - 1)$  eigenvalues corresponding to the rest oscillators at  $\exp(\pm i2\pi\omega_0/\omega_b)$  and two at  $+1$  corresponding to the excited one. For a dark breather at the anticontinuous limit there are  $2(N - 1)$  eigenvalues at  $+1$ , and a couple of conjugate eigenvalues at  $\exp(\pm i2\pi\omega_0/\omega_b)$ .

Figure 1 shows the Floquet multipliers for both a bright and a dark breather at the anti-continuous limit  $\varepsilon = 0$ . When the coupling  $\varepsilon$  is switched on, these eigenvalues move on the complex plane as continuous functions of  $\varepsilon$ , and an instability can be produced only in three different ways [1]: (a) a couple of conjugate eigenvalues reaches the value  $1 + 0i$  ( $\theta = 0$ ) and leaves the unit circle along the real line (harmonic bifurcation); (b) a couple of conjugate eigenvalues reaches  $-1$  ( $\theta = \pm\pi$ ) and leaves the unit circle along the real line (subharmonic bifurcation); (c) two pairs of conjugate eigenvalues collide at two conjugate points on the unit circle and leave it (Krein crunch or oscillatory bifurcation). It must be remembered that a bifurcation involving two eigenvalues with the same sign of the Krein signature  $\kappa(\theta) = \text{sign}(i(\dot{\xi} \cdot \xi^* - \dot{\xi}^* \cdot \xi))$  is not possible [1].

The basic features of the Floquet multipliers at the anti-continuous limit for bright and dark breathers are the following:

- For bright breathers, there are  $N - 1$  Floquet multipliers corresponding to the oscillators at rest. They are degenerated at  $\theta = \pm 2\pi\omega_0/\omega_b$ . The eigenvalues at  $0 < \theta < \pi$  have  $\kappa > 0$  while the ones at  $-\pi < \theta < 0$  have  $\kappa < 0$ . If  $\theta = 0$  or  $\pi$   $\kappa = 0$ . In addition, there are two eigenvalues at  $1 + 0i$ , corresponding to the excited oscillator.

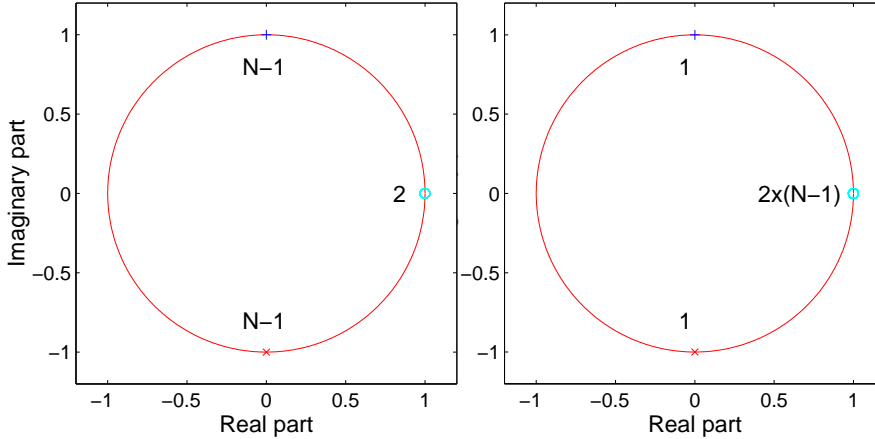


**Figure 1.** Floquet multipliers at zero coupling for: (left) a bright breather and (right) a dark breather with the numbers of identical multipliers.

- For dark breathers, there are two eigenvalues at  $\theta = \pm 2\pi\omega_0/\omega_b$  corresponding to the oscillator at rest, and there are  $2(N - 1)$  eigenvalues at  $1 + 0i$  corresponding to the excited oscillators.

When the coupling is switched on, the evolution of the Floquet multipliers for bright breathers is rather different from the case of dark breathers:

- For a bright breather, the Floquet eigenvalues corresponding to the oscillators at rest lose their degeneracy and expand on two bands of eigenvalues, called the phonon bands. Their corresponding eigenmodes are extended. These two bands move on the unit circle and eventually cross each other. In this case, eigenvalues of different Krein signature can collide and abandon the unit circle through subharmonic or oscillatory bifurcations. In addition, some eigenvalues can abandon the bands and become localized [23]. A pair of complex conjugate eigenvalues can collide at  $1 + 0i$  leading to a harmonic bifurcation or collide with the phonon band through an oscillatory bifurcation.
- For a dark breather, the eigenvalues corresponding to the excited oscillators, with extended phonon eigenmodes, can either depart from the unit circle along the real axis (harmonic bifurcation) or move along the unit circle. In the last case, they can collide with the eigenvalue corresponding to the rest oscillator (with localized eigenmode) through a Krein crunch. Eventually, if the on-site potential is non-symmetric, the eigenvalues collide at  $-1 + 0i$ , leading to a cascade of subharmonic bifurcations.

The study of breather stability can be complemented by means of Aubry's band theory [1]. It consists in studying the linearized system (8) for  $E \neq 0$ , with the corresponding family of Floquet operators  $\mathcal{F}_E$ . For each operator  $\mathcal{F}_E$  there are  $2 \times N$

Floquet multipliers. A Floquet multiplier can be written as  $\lambda = \exp(i\theta)$ .  $\theta$  is called the Floquet argument. If  $\theta$  is real then  $|\exp(i\theta)| = 1$  and the corresponding eigenfunction of (8) is bounded and corresponds to a stability mode; if  $\theta$  is complex, it corresponds to an instability mode. The set of points  $(\theta, E)$ , with  $\theta$  real, has a band structure. The breather is stable if there are  $2 \times N$  band intersections (including tangent points with their multiplicity) with the axis  $E = 0$ . The bands are reduced to the first Brillouin zone  $(-\pi, \pi]$  and are symmetric with respect to the axis  $\theta = 0$ . The fact that  $\mathcal{F}_0$  has always a double  $+1$  eigenvalue corresponding to the phase mode  $\dot{u}(t)$  manifests as a band which is tangent to the  $E = 0$  axis.

For the uncoupled system, the structure of the stable and unstable bands is completely explained by the theory (although it has to be calculated numerically). For the coupled system, such structure is expected to change in a continuous way in terms of the parameter  $\varepsilon$ . We will use band theory, to predict the evolution of the eigenvalues of  $\mathcal{F}_0$ , with a model parameter is changed.

At zero coupling, the bands corresponding to the oscillators at rest can be analytically calculated from the equation:

$$\ddot{\xi}_n + \omega_0^2 \xi_n = E \xi_n, \quad (11)$$

they are given by  $E = \omega_0^2 - \omega_b^2 \theta^2 / (2\pi)^2$ . The bands corresponding to the  $N - 1$  excited oscillators are a deformation of the band corresponding to the oscillator at rest (which will be called *rest bands*) and one of them must be tangent to  $E = 0$  axis at  $(\theta, E) = (0, 0)$  [1]. The bands are bounded from above and numbered starting from the top, being the 0th band the first one. If the on-site potential is soft the 1st band will be tangent to the  $E = 0$  axis at  $(0, 0)$  with positive curvature. If the on-site potential is hard, the tangent band at  $(0, 0)$  will be the 2nd one, and will have negative curvature [21]. At the anticontinuous limit the band scheme of a bright and a dark breather are similar, differing only in the number of bands that corresponds to the oscillators at rest or to the excited oscillators (*excited bands*) as it is shown in Figures 2 and 3.

The bright breather has only one band tangent to the axis  $E = 0$  and that band cannot leave this position because, when the coupling is switched on, there must be a tangent band corresponding to the phase mode. The situation is totally different for a dark breather: there are  $N - 1$  bands tangent to the  $E = 0$  axis and  $N - 2$  of them can move without any restriction. If some of them move upwards, the intersection points disappear, which implies that some Floquet arguments become complex or, equivalently, that some Floquet multipliers abandon the unit circle and the breather becomes unstable.

## 5. Dark breathers with soft on-site potentials

Let us consider a model with a cubic on-site potential given by

$$V(u_n) = \frac{1}{2} \omega_0^2 u_n^2 - \frac{1}{3} u_n^3, \quad (12)$$

that is,  $\phi'(u_n) = -u_n^2$  in the dynamical equations (4). Figure 4 represents the Floquet multipliers for  $\varepsilon \neq 0$ . The left side of the figure shows the Floquet multipliers of a stable bright breather for a coupling  $\varepsilon = 0.1$ . However, as can be seen at the right side of the figure, the dark breather experiences a multiple harmonic bifurcation as soon as the coupling is switched on. Therefore, for a lattice with a cubic on-site potential

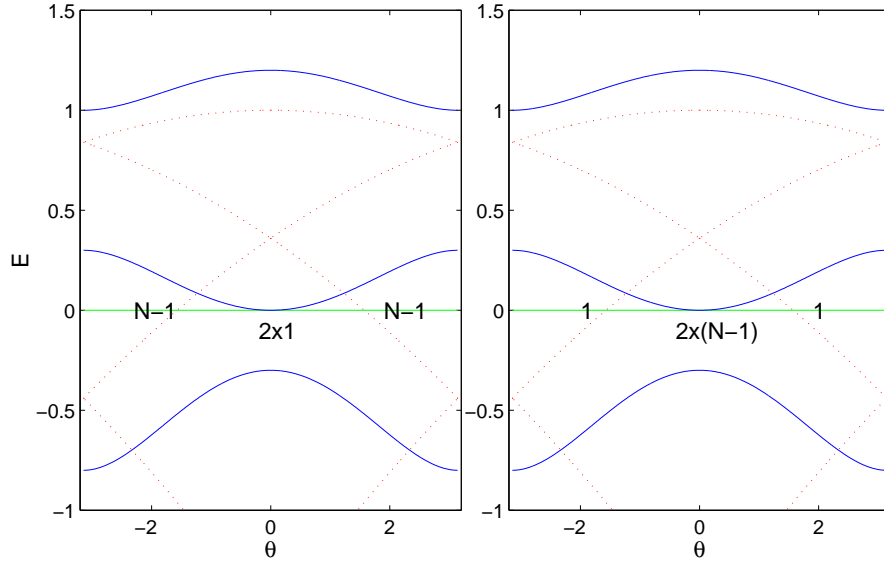


**Figure 2.** Band scheme for bright (left) and dark (right) breathers with soft potential. The continuous lines correspond to the excited oscillators and are numbered downwards starting from zero. The dotted lines correspond to the oscillator at rest.

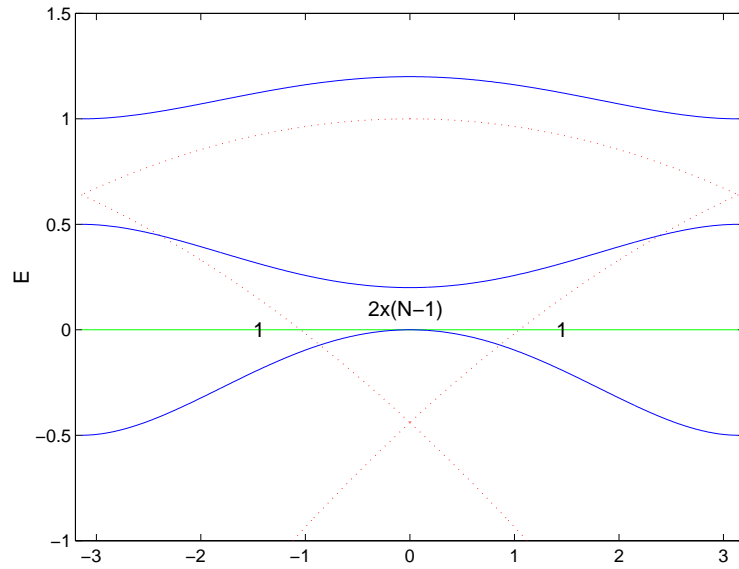


**Figure 3.** Bands scheme for a dark breather with hard potential at zero coupling. The continuous lines correspond to the excited oscillators and are numbered downwards starting from zero. The dotted lines correspond to the oscillator at rest.



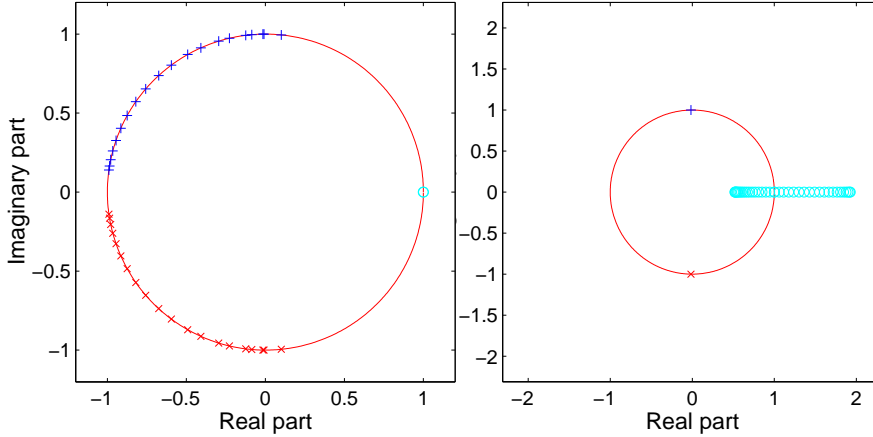


**Figure 4.** Evolution of the Floquet multipliers with cubic on-site potential and attractive interaction when the coupling is switched on for: (left) the bright breather at  $\varepsilon = 0.1$ , which is linearly stable, although reaching a possible bifurcation at  $-1$ ; (right) the dark breather at a much smaller coupling parameter  $\varepsilon = 0.004$ . The breather frequency is  $\omega_b = 0.8$ .

and attractive interaction, dark breathers exist but they are unstable for every value of the coupling.

This problem can be investigated by means of Aubry's band analysis. It has given us an explanation for the previous behaviour and also a guide for modifying the model in order to obtain stable dark breathers. The bands at zero coupling can be seen in Figure 5.

As it is explained above and shown in Figure 4, the cubic dark breather becomes unstable for any attractive coupling  $\varepsilon > 0$  through harmonic bifurcations. This is easily understood in terms of the band structure:  $N - 2$  tangent bands move upwards, which is mathematically demonstrated in Ref. [24]. They lose the tangent points with the  $E = 0$  axis as Figure 6 shows. Therefore, in order that the breather can be stable all the excited bands except one have to move downwards, transforming the points tangent to the  $E = 0$  axis into intersection points. A straightforward alternative is to change the sign of the parameter  $\varepsilon$  in (1). This is equivalent to using a dipole-dipole coupling potential  $W(u) = \sum_n u_{n+1} u_n$ , i.e., the Hamiltonian can be written as:

$$H = \sum_n \left( \frac{1}{2} \dot{u}_n^2 + \frac{1}{2} \omega_0^2 u_n^2 - \frac{1}{3} u_n^3 + \frac{1}{2} \varepsilon (u_{n+1} u_n) \right) \quad (13)$$

with  $\varepsilon > 0$ . This repulsive interaction has been used recently to model DNA-related models [25, 26, 27, 28, 29, 30]. The dynamical equations with repulsive interaction and cubic on-site potential become:

$$\ddot{u}_n + \omega_0^2 u_n - u_n^2 + \varepsilon (u_{n-1} + u_{n+1}) = 0, \quad (14)$$

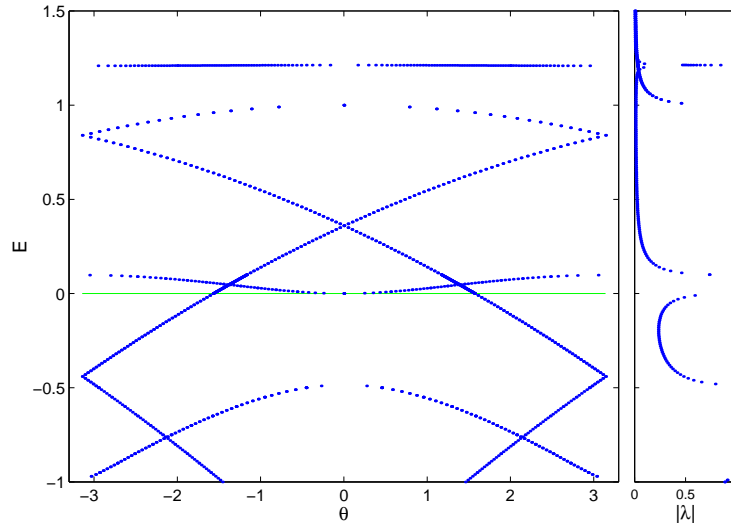


**Figure 5.** Band structure at zero coupling for a cubic on-site potential. The right part of the figure plots the moduli of the unstable Floquet multipliers that are smaller than 1, being their inverses the unstable multipliers. Frequency  $\omega_b = 0.8$

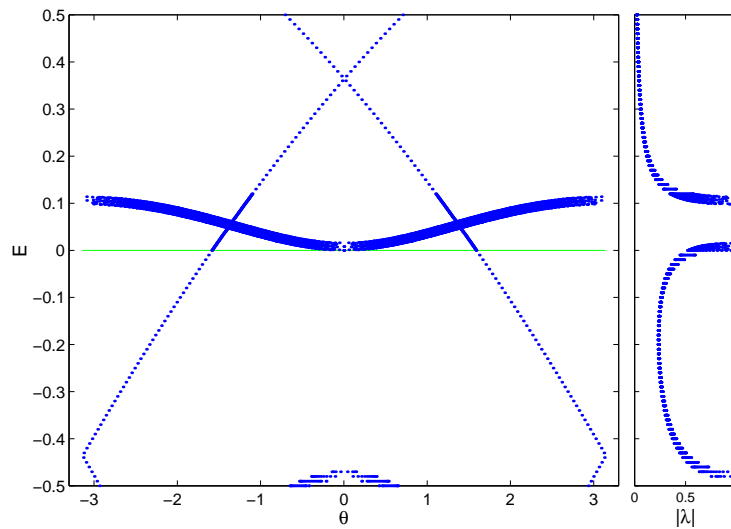


**Figure 6.** Band structure of a dark breather with cubic on-site potential and attractive interaction at very low coupling ( $\varepsilon = 0.004$ ). Frequency  $\omega_b = 0.8$ .

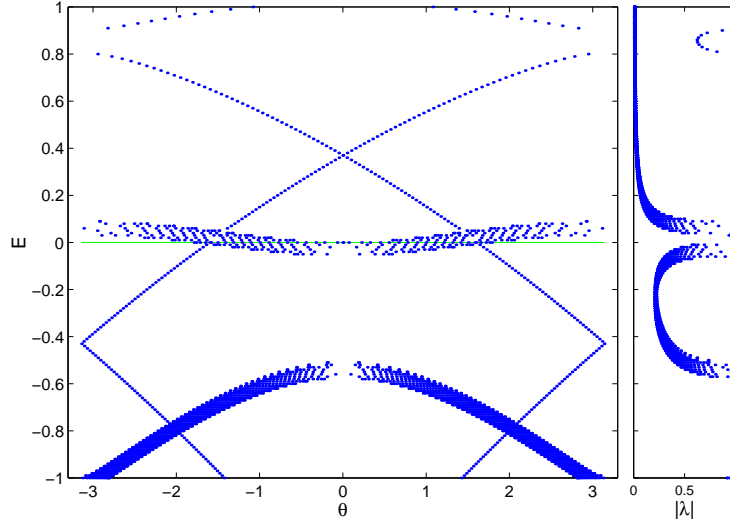


**Figure 7.** Band structure of a dark breather with cubic on-site potential and repulsive interaction at  $\varepsilon = 0.015$ . Frequency  $\omega_b = 0.8$ .

and the linear stability equations become:

$$\ddot{\xi}_n + \omega_0^2 \xi_n - 2u_n \xi_n + \varepsilon(\xi_{n-1} + \xi_{n+1}) = 0. \quad (15)$$

Figure 7 displays the band structure at  $\varepsilon = 0.015$  for this system. The  $N-2$  bands that are allowed to move will perform a downwards movement and therefore the breather is stable.

A further increase of  $\varepsilon$  leads to Krein crunches. They are caused by the mixing of the rest bands and the excited bands, that produces “wiggles” in the excited bands and gaps appears between them [31]. When these bands move downwards and the “wiggles” cross the  $E = 0$  axis, intersection points are lost but recovered when the coupling increases. It manifests as the appearance of “instability bubbles”. These instabilities depend on the size of the system, as will be shown in section 7. The system will eventually become unstable through a cascade of subharmonic bifurcations when the lower excited band goes below the  $E = 0$  axis, losing the intersection points at  $\theta = \pm\pi$  (see figure 8).

We have obtained dark breathers for systems with cubic on-site potential and attractive or repulsive interaction even though dark breathers with attractive coupling are not stable. Figure 9 shows two different examples of dark breathers for this two types of coupling. Notice that the oscillator with small amplitude is in phase with its neighbours when the system is unstable (left) while is in anti-phase when it is stable (right).

This type of behaviour is general for other soft on-site potentials as it can be obtained using, for example, the Morse potential given by

$$V(u_n) = D(\exp(-bu_n) - 1)^2. \quad (16)$$

For this system, dark breathers maintain their stability until the coupling parameter reaches the value  $\varepsilon = 0.024$ . From this value Krein bifurcations appear. These bifurcations are harmless in the sense that they preserve the dark localization, but

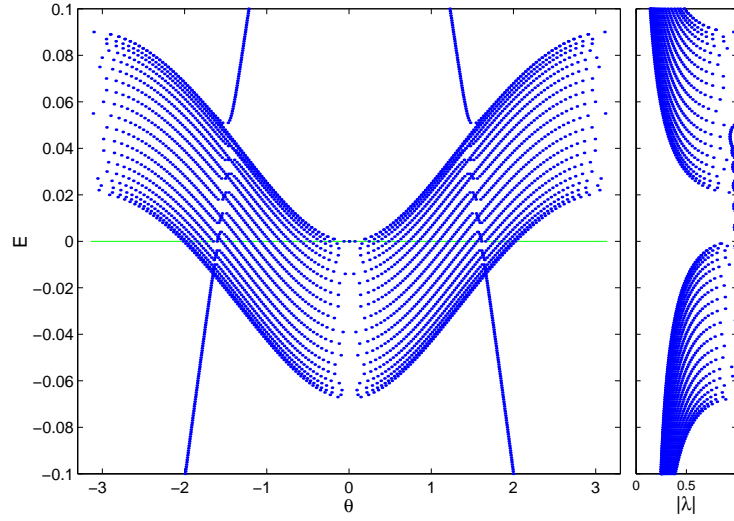


**Figure 8.** Band structure of a dark breather with cubic on-site potential and repulsive interaction at  $\varepsilon = 0.017$  and  $\omega_b = 0.8$ . Note the “wiggles” that appear when the excited bands and the rest band mix. A further increase of the coupling parameter  $\varepsilon$  will make the excited bands fall below  $E = 0$  producing subharmonic bifurcations.

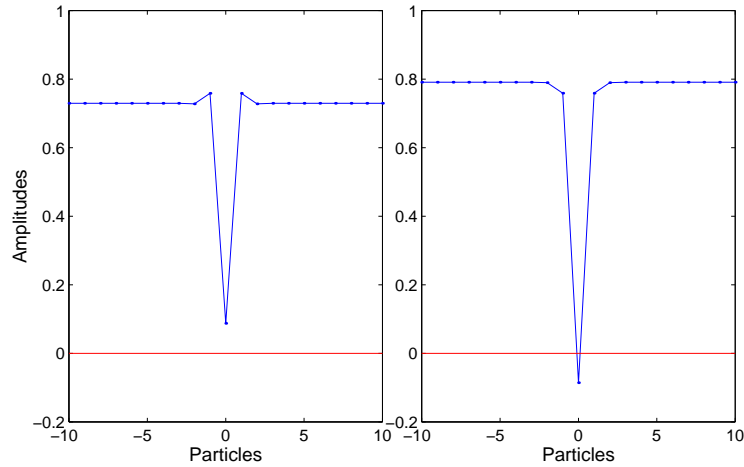


**Figure 9.** Dark breathers profile for a cubic potential with attractive interaction (left) and with repulsive interaction (right), at  $\varepsilon = 0.023$ . The last one is stable.

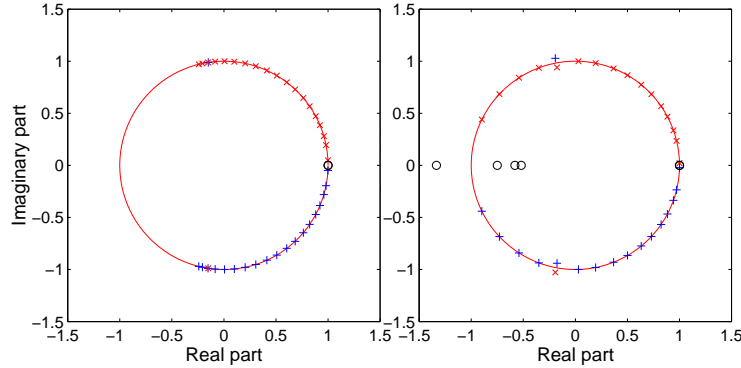


**Figure 10.** Evolution of the Floquet eigenvalues for a Morse on-site potential and repulsive coupling. Left:  $\varepsilon = 0.024$ , the system is still stable. Right:  $\varepsilon = 0.035$ , the system becomes unstable due to subharmonic bifurcation and Krein crunches.

the breather becomes quasiperiodic with a superimposed frequency to the breather one. For  $\varepsilon > 0.033$ , the system becomes unstable due to subharmonic bifurcations. Figure 10 shows this behaviour in terms of the corresponding Floquet multipliers for two different values of the coupling. With this potential, it has been described [11] that for values of the  $\omega_b$  close to the linear frequency  $\omega_0$  (in fact, slightly above it), oscillatory instabilities can bring about the movement of dark breathers, when the corresponding eigenvalue is asymmetric and localized. It does not happen for frequencies far enough of  $\omega_0$  as the ones of the order we present here.

An interesting variation of this scheme occurs if we consider symmetric on-site potentials as the quartic soft potential given by

$$V(u_n) = \frac{1}{2} \omega_0^2 u_n^2 - \frac{1}{4} u_n^4. \quad (17)$$

In this case the potential is symmetric and no subharmonic bifurcations at  $\lambda = \pm 1$  occur because the bands are gapless at  $\theta = \pm\pi$ . This characteristic enlarges the stability range (see Figure 11). The system eventually becomes unstable (apart from the reentrant instabilities due to Krein crunches) through harmonic bifurcations.

## 6. Dark breathers with hard on-site potentials

The band scheme of a system with hard on-site potential at  $\varepsilon = 0$  is shown in Figure 3. There are  $N - 1$  bands tangent to the axis  $E = 0$ . It is clear that the breather will remain stable provided that the tangent bands keep the intersection points when the degeneracy is raised with  $\varepsilon \neq 0$ . In this system it means that the  $N - 2$  bands that can move will perform an upwards movement. Therefore, the dark breather will be stable with an attractive coupling potential. We have used for the numerics the quartic hard on-site potential, that is

$$V(u_n) = \frac{1}{2} \omega_0^2 u_n^2 + \frac{1}{4} u_n^4. \quad (18)$$

The Hamiltonian is then

$$H = \sum_n \left( \frac{1}{2} \dot{u}_n^2 + \frac{1}{2} \omega_0^2 u_n^2 + \frac{1}{3} u_n^3 + \frac{1}{2} \varepsilon (u_{n+1} - u_n)^2 \right) \quad (19)$$

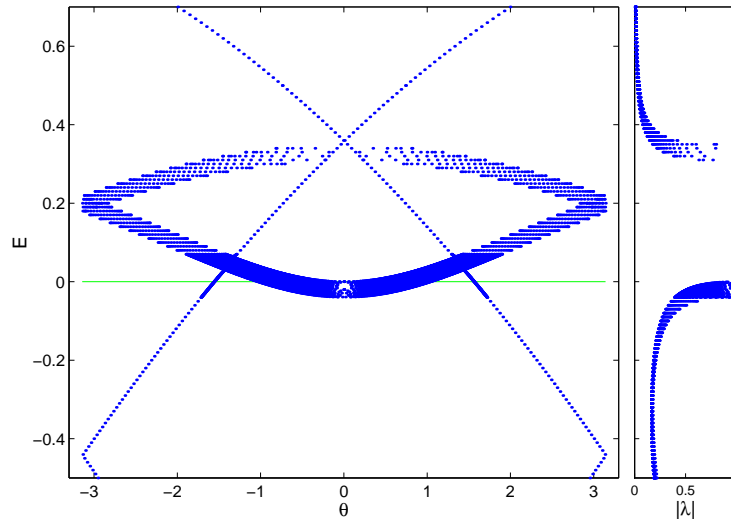


**Figure 11.** Band structure for a dark breather with quartic soft on-site potential and repulsive coupling. Note the absence of gaps at  $\theta = \pm\pi$  which enlarges the stability range. Parameters:  $\varepsilon = 0.018$  and  $\omega_b = 1.2$ .

Figure 12 shows that at  $\varepsilon = 0.01$  the tangent bands have moved upwards and, therefore, the stability of the system is maintained. The system loses its stability at  $\varepsilon = 0.022$  where a harmonic bifurcation appears. The instability mode, shown in 14 with its multipliers, is an asymmetric extended one. Simulations done perturbing with it the dark breather give rise to a small oscillation with both sides of the chain out of phase, superimposed to the dark breather one, but the *darkness* is preserved. After that, there are Krein crunches due to the bands mixing with the usual properties.

## 7. Finite size effects

This final section is dedicated to comment some preliminary results relative to the finite size effects on instability of dark breathers. Important differences appear with respect to the case of bright breathers [31].

In the case of bright breathers, there are two kinds of size-dependent bifurcations. The origin of them relies on the nature of the localization of the colliding eigenvalues. If the colliding eigenvalues are extended, there appear “instability bubbles”, i.e. the Floquet eigenvalues abandon the unit circle after the collision but return afterwards. These bifurcations disappear when the system is infinite. Alternatively, a localized eigenvalue can collide with a band of extended eigenvalues. In this case, the instability bubbles also occur but they persist even though the system is infinite.

In order to study the case of dark breathers, we have chosen a Morse on-site potential with repulsive interaction. As a result of this analysis, the collision of extended eigenvalues always implies a cascade of subharmonic bifurcations (see section 4) independently of the size of the system. It is due to the fact that they are due to excited bands, whose Floquet arguments belong to the first Brillouin zone, losing intersections at  $\theta = \pi$ . It is different from the case of bright breathers where this kind

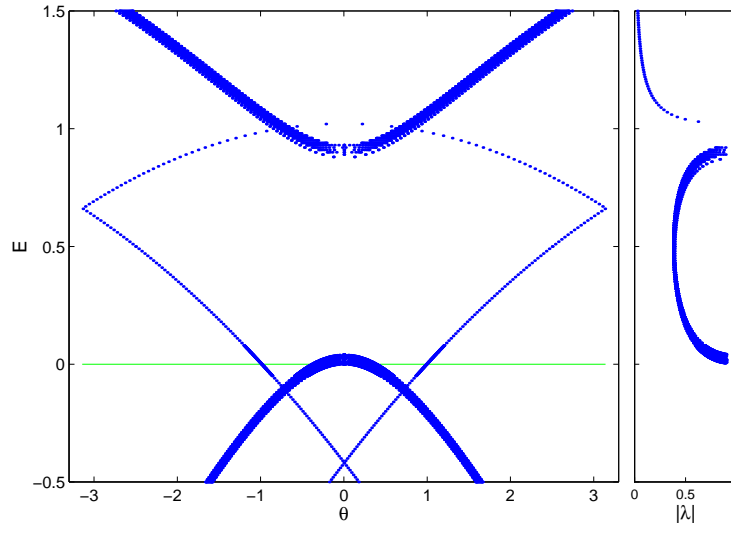


**Figure 12.** Band structure for a quartic hard on-site potential with attractive interaction at  $\varepsilon = 0.01$  and  $\omega_b = 1.2$ .

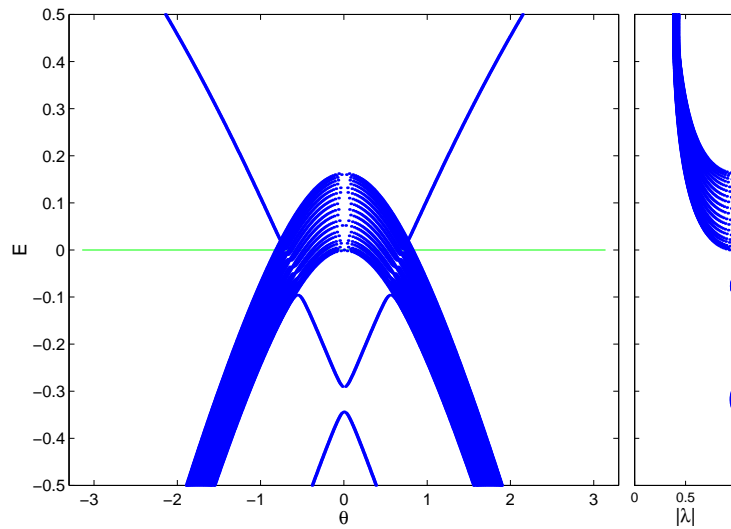


**Figure 13.** Zoom of the band structure for a quartic hard on-site potential with attractive interaction at  $\varepsilon = 0.041$  and  $\omega_b = 1.2$ .

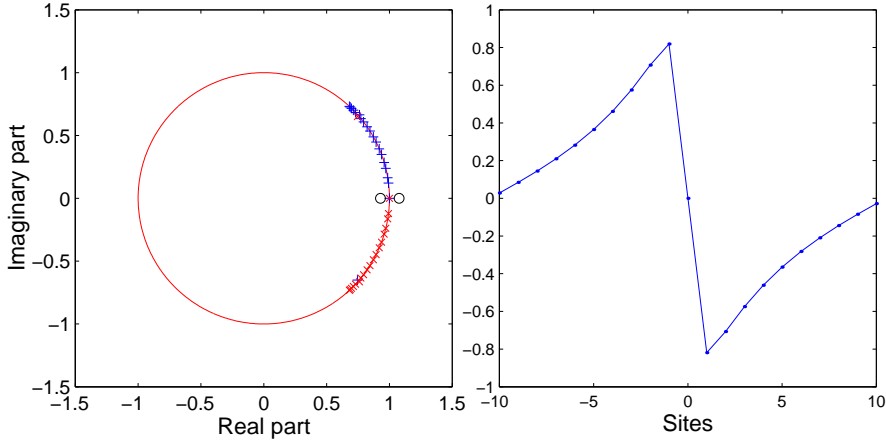


**Figure 14.** Left: Floquet multipliers with a quartic hard on-site potential and attractive interaction at  $\varepsilon = 0.041$  and  $\omega_b = 1.2$ . A harmonic and a small Krein instabilities appear. Right: the velocities components (the position ones are zero) of the eigenvalue corresponding to the harmonic instability.

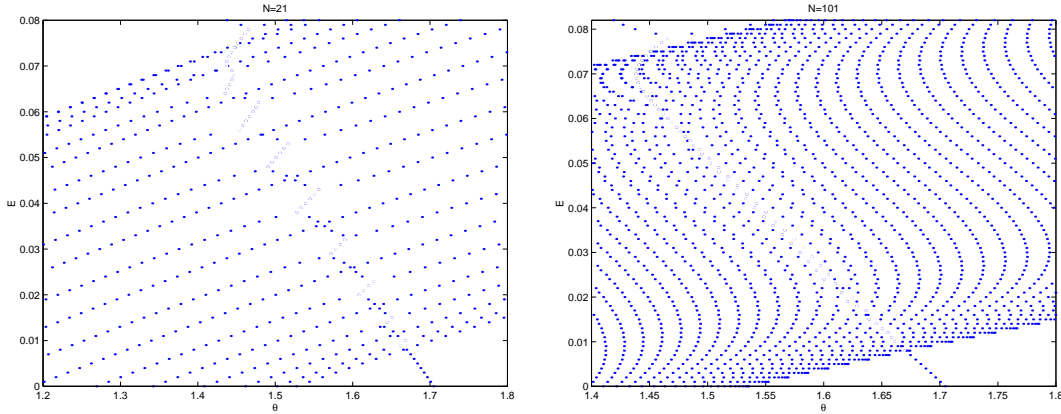


**Figure 15.** Zoom of the band scheme for  $N=21$  and  $N=101$  and a Morse potential ( $\varepsilon = 0.02$  and  $\omega_b = 0.8$ ). It can be observed the appearance of wiggles when  $N=21$ , which are much wider when  $N=101$  these wiggles are almost invisible because they occupy the width of the band.

of instabilities are due to modes corresponding to oscillators at rest and the bands must be reduced to the first Brillouin zone.

Also, an eigenvalue corresponding to an extended mode can collide with a localized mode. In this case, the rest (localized mode) band and the excited (extended modes) bands mix (see Figures 15). There appear “wiggles” that imply the opening of gaps in the band scheme, which are the origin of the instability bubbles. However, when the size of the system is increased, the wiggles widen until they occupy almost the width of the quasi-continuous extended mode bands. This fact implies that, although the instability bubbles disappear, the Krein crunches are unavoidable (see Figure 16). Nevertheless, the breathers are robust despite of the existence of these instabilities.



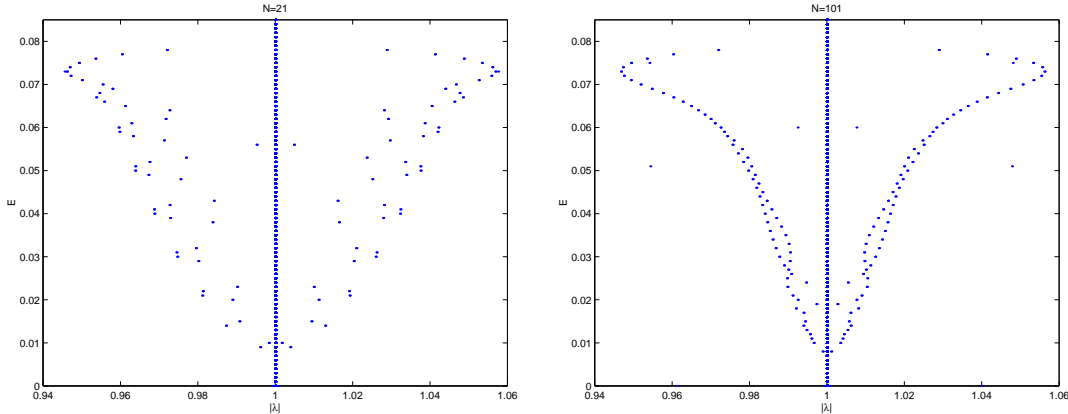


**Figure 16.** Moduli of the Floquet eigenvalues corresponding to the Krein crunches for  $N=21$  and  $N=101$  and a Morse potential ( $\varepsilon = 0.02$  and  $\omega_b = 0.8$ ). It can be observed the appearance of instability bubbles when  $N=21$ . However, these bubbles transform into an instability that persist up to a value of the coupling for which the breather is unstable because of the subharmonic bifurcations.

## 8. Dark breathers stability in dissipative systems

There appear some important differences in the study of the stability of dark breathers in dissipative systems with respect to the Hamiltonian case.

In order to perform this study, we start from the dissipative Frenkel–Kontorova model [32]:

$$\ddot{u}_n + \gamma \dot{u}_n + V'(u_n) + \varepsilon(2u_n - u_{n+1} - u_{n-1}) = F \sin \omega_b t. \quad (20)$$

where  $\gamma$  is a damping parameter and  $F$  the amplitude of an external force.

In the anticontinuous limit, there are no band tangent to the  $E = 0$ -axis (figure 17a). It implies that, when the coupling is introduced, there are no losing of intersections of the bands with independence of the sign of the coupling constant ( $\varepsilon$ ). Furthermore, the band corresponding to the oscillator at rest do not mix with the band of the background and oscillatory instabilities do not appear. These phenomena are shown in figure 17.

## 9. Conclusions

In this paper we have explored the existence and stability of dark breathers in one-dimensional Klein–Gordon models, for frequencies far enough from the linear frequencies to the DNLS approximation be justified. We have found stable dark breathers in several types of them. For systems with soft on-site potential, there are no stable dark breathers if the coupling between particles is attractive, but with a repulsive coupling the stability is assured for fairly high values of the coupling parameter  $\varepsilon$ . As  $\varepsilon$  increases instability bifurcations due to Krein crunches take place as a consequence of the band mixing between the rest oscillator band and the dark background. Eventually, the system experiences subharmonic bifurcations at  $-1$  that make the breather unstable. If the soft on-site potential is symmetric the subharmonic bifurcations are avoided and the final instability is caused by harmonic bifurcations.

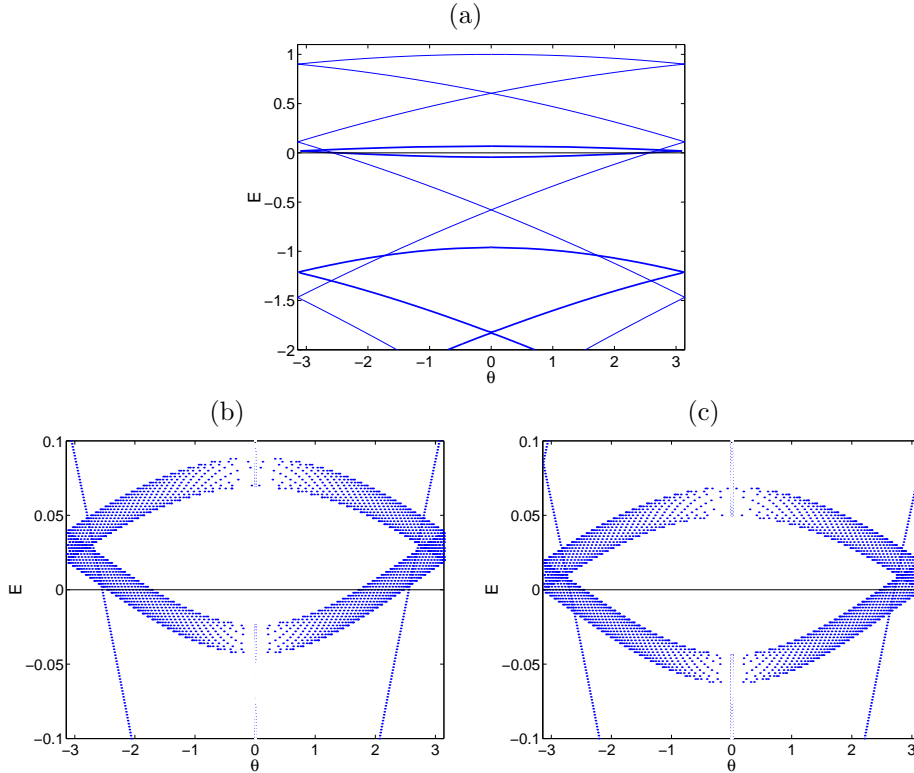


**Figure 17.** Band diagrams in the anticontinuous limit (top) and for a coupling  $\varepsilon = \pm 0.005$  (bottom) for a dark breather in the Frenkel–Kontorova model. The parameters are:  $\omega_b = 0.2\pi$ ,  $\gamma = 0.02$  y  $F = 0.02$ . (b) corresponds to an attractive interaction potential, whereas (c) corresponds to a repulsive potential. The dark breather is stable in both cases.

For systems with hard on-site potentials, the situation is reversed and the dark breathers are stable with attractive coupling and unstable with repulsive one. They experience harmonic bifurcations at  $+1$  apart from the Krein crunches. An analysis of larger systems shows that these bifurcations persist even though the system is infinite. Dissipative systems are, however, stable for both types of coupling.

We are now on the project of performing a wider study of dark breathers in dissipative systems. Another interesting aspect is to study the relationship of the vibration pattern of dark breathers with the hardness of the on-site potential and the type of coupling. The ansatz  $u_n \rightarrow (-1)^n u_n$ , which transforms repulsive coupling into attractive one and vice versa, for symmetric potentials, suggests, and it has been shown for the DNLS equations, and we also have checked numerically, that the stability conditions are reversed are low coupling, but the bifurcations for  $|\omega_b - \omega_0|$  large enough, highly asymmetric potentials as found in chemical and biological systems, and larger coupling are worth studying.

## Acknowledgments

This work has been supported by the European Union under the RTN project, LOCNET, HPRN-CT-1999-00163.

JFR Archilla acknowledges Informatics and Mathematical Modelling at DTU for hospitality, while this work was started and Yu B Gaididei for valuable suggestions.

J Cuevas acknowledges an FPDI grant from ‘La Junta de Andalucía’.

- [1] S Aubry. Breathers in nonlinear lattices: Existence, linear stability and quantization. *Physica D*, 103:201–250, 1997.
- [2] S Flach and CR Willis. Discrete breathers. *Physics Reports*, 295:181–264, 1998.
- [3] RS MacKay and S Aubry. Proof of existence of breathers for time-reversible or Hamiltonian networks of weakly coupled oscillators. *Nonlinearity*, 7:1623–1643, 1994.
- [4] JL Marín and S Aubry. Breathers in nonlinear lattices: Numerical methods based on the anti-integrability concept. In L Vázquez, L Streit, and VM Pérez-García, editors, *Nonlinear Klein-Gordon and Schrödinger Systems: Theory and Applications*, pages 317–323. World Scientific, Singapore and Philadelphia, 1995.
- [5] VE Zakharov and AB Shabat. Exact theory of two-dimensional self-focusing and one-dimensional self-modulation of waves in nonlinear media. *Sov. Phys. JETP*, 34:62–69, 1972.
- [6] VE Zakharov and AB Shabat. Interaction between solitons in a stable medium. *Sov. Phys. JETP*, 37:823, 1973.
- [7] YuS Kivshar and M Peyrard. Modulational instabilities in discrete lattices. *Phys. Rev. A*, 46:3198, 1992.
- [8] YuS Kivshar, W Królikowski, and OA Chubykalo. Dark solitons in discrete lattices. *Phys. Rev. E*, 50(6):5020–5032, 1994.
- [9] VV Konotop and S Takeno. Stationary dark localized modes: Discrete nonlinear Schrödinger equations. *Phys. Rev. E*, 60(1):1001–1008, 1999.
- [10] M Johansson and YuS Kivshar. Discreteness-induced oscillatory instabilities of dark solitons. *Phys. Rev. Lett.*, 82:85, 1999.
- [11] AM Morgante, M Johansson, G Kopidakis, and S Aubry. Standing waves instabilities in a chain of nonlinear coupled oscillators. *Phys. D*, 162:53, 2002.
- [12] B Denardo, B Gakvin, A Greenfield, A Larraza, and S Puttermann. Observations of localized structures in nonlinear lattices: Domain walls and kinks. *Phys. Rev. Lett.*, 68:1730, 1992.
- [13] R. Dusi and M. Wagner. Gauss procedure for the construction of self-localized solitons in discrete systems. *Phys. Rev. B*, 51(22):15847–15855, 1995.
- [14] I. Daumont, T. Dauxois, and M. Peyrard. Modulational instability: first step towards energy localization in nonlinear lattices. *Nonlinearity*, 10:617–630, 1997.
- [15] M Peyrard and AR Bishop. Statistical-mechanics of a nonlinear model for DNA denaturation. *Phys. Rev. Lett.*, 62(23):2755–2758, 1989.
- [16] S Flach. Existence of localized excitations in nonlinear Hamiltonian lattices. *Phys. Rev. E*, 51(2):1503–1507, 1995.
- [17] S Flach. Obtaining breathers in nonlinear Hamiltonian lattices. *Phys. Rev. E*, 51(4):3579–3587, 1995.
- [18] JL Marín and S Aubry. Breathers in nonlinear lattices: Numerical calculation from the anticontinuous limit. *Nonlinearity*, 9:1501–1528, 1996.
- [19] JL Marín, S Aubry, and L. M. Floría. Intrinsic localized modes: discrete breathers. existence and linear stability. *Physica D*, 113:283–292, 1998.
- [20] RS MacKay and JA Sepulchre. Stability of discrete breathers. *Physica D*, 119:148–162, 1998.
- [21] JL Marín. *Intrinsic Localised Modes in Nonlinear Lattices*. PhD dissertation, University of Zaragoza, Department of Condensed Matter, June 1997.
- [22] J. M. Sanz-Serna and M. P. Calvo. *Numerical Hamiltonian Problems*. Chapman and Hall, 1994.
- [23] C Baesens, S Kim, and RS MacKay. Localised modes on localised equilibria. *Physica D*, 113:242–247, 1998.
- [24] B Sánchez-Rey JFR Archilla, J Cuevas and A Alvarez. To be submitted.
- [25] PL Christiansen, Yu B Gaididei, M Johansson, KØ Rasmussen, VK Mezentsev, and JJ Rasmussen. Solitary excitations in discrete two-dimensional nonlinear Schrödinger models with dispersive dipole-dipole interactions. *Phys. Rev. B*, 57(18):11303–11318, 1998.
- [26] YB Gaididei, SF Mingaleev, and PL Christiansen. Curvature-induced symmetry breaking in nonlinear Schrödinger models. *Phys. Rev. E*, 62(1):R53–R56, 2000.
- [27] JFR Archilla, PL Christiansen, and Yu B Gaididei. Interplay of nonlinearity and geometry in

- a DNA-related, Klein-Gordon model with long-range dipole-dipole interaction. *Phys. Rev. E*, 65(1):016609–016616, 2001.
- [28] PL Christiansen, YuB Gaididei, and SF Mingaleev. Effects of finite curvature on soliton dynamics in a chain of nonlinear oscillators. *J. Phys. Condens. Matter*, 13(6):1181–1192, 2001.
- [29] J Cuevas, JFR Archilla, Yu B Gaididei, and FR Romero. Static and moving breathers in a DNA model with competing short- and long-range dispersive interactions. *Physica D*, 163:106–126, 2002.
- [30] J Cuevas, F Palmero, JFR Archilla, and FR Romero. Moving breathers in a bent DNA-related model. *Phys. Lett. A*, 2002. Submitted.
- [31] JL Marín and S Aubry. Finite size effects on instabilities of discrete breathers. *Physica D*, 119:163–174, 1998.
- [32] JL Marn, F Falo, PJ Martinez, and LM Flora. Discrete breathers in dissipative lattices. *Phys. Rev. E*, 63:066603, 2001.